

Environmental drivers of historical grain price variations in Europe

Jan Esper^{1,*}, Ulf Büntgen^{2,3,4}, Sebastian Denzer¹, Paul J. Krusic^{5,6}, Jürg Luterbacher^{7,8}, Regina Schäfer⁹, Rainer Schreg¹⁰, Johannes Werner¹¹

¹Department of Geography, Johannes Gutenberg University, 55099 Mainz, Germany

²Department of Geography, University of Cambridge, Cambridge CB2 3EN, UK

³Swiss Federal Research Institute WSL, 8903 Birmensdorf, Switzerland

⁴Global Change Research Centre and Masaryk University, Brno, Czech Republic

⁵Department of Physical Geography, Stockholm University, 10691 Stockholm, Sweden

⁶Navarino Environmental Observatory, 24001 Messinia, Greece

⁷Department of Geography, Justus Liebig University, 35390 Giessen, Germany

⁸Centre for International Development and Environmental Research, Justus Liebig University, 35390 Giessen, Germany

⁹Department of History, Johannes Gutenberg University, 55122 Mainz, Germany

¹⁰Römisch-Germanisches Zentralmuseum, 55116 Mainz, Germany

¹¹Bjerknes Centre for Climate Research and Department of Earth Science, University of Bergen, 5020 Bergen, Norway

ABSTRACT: Grain price (GP) volatility has been a central constituent of European commerce, with fluctuations in barley, rye and wheat prices having been carefully documented over centuries. However, a thorough understanding of the climatic and environmental drivers of long-term GP variations is still lacking. Here, we present a network of historical GP records from 19 cities in central and southern Europe for the 14th to 18th centuries. Spatial variability at interannual to multidecadal scales within this network was compared with reconstructed warm-season temperatures and hydroclimatic conditions. We show that European GPs are tightly coupled with historical famines and that food shortages coincide with regional summer drought anomalies. Direct correlations between historical GP and reconstructed drought indices are low, hardly exceeding $r = -0.2$. Yet if the analysis is focused on extreme events, the climatic controls on high-frequency price variations become obvious: GPs were exceptionally high during dry periods and exceptionally low during wet periods. In addition, we find that GP variations were affected by temperature fluctuations at multidecadal timescales. The influence of summer temperatures is particularly strong over the 1650–1750 period, subsequent to the Thirty Years' War, reaching $r = -0.40$ at the European scale. This observation is supported by the lack of correlation among regional GP clusters during the period of hostilities and increased inter-regional correlation thereafter. These results demonstrate that the exchange of goods and spatial coherence of GP data in Europe were controlled both by socio-political and environmental factors, with environmental factors being more influential during peacetime.

KEY WORDS: Historic volatility · Climate signal · Thirty Years' War · Drought · Temperature · Reconstruction

— Resale or republication not permitted without written consent of the publisher —

1. INTRODUCTION

The causes and consequences of historical grain price (GP) volatility in Europe have been thoroughly analyzed over the past several decades (Braudel & Spooner 1967, Van der Wee 1978, de Vries 1980, Post 1985, Söderberg 2006, Campbell & Ó Gráda 2011).

Grain is one of the most important markets and barley, rye and wheat prices have carefully been documented in many European cities since late medieval times (Allen 2001). Studies of historical GP volatility have helped towards further understanding of market performance and failure, and evaluate the effects of market liberalization and links to political authori-

tarianism (Persson 1999). Historical GP data have been used to disclose the significance of harvest shocks on local populations and document the effects of market integration through trade caused by falling transport costs (Pfister et al. 2011). Evidence from economic history indicates that the combination of harvest shocks and poor market integration is the most influential driver of historical GP rises (Persson 1999 and references therein).

Historians and geoscientists have long known that GP records contain information on varying ecological boundary conditions that could improve our understanding of past environmental changes (Glaser 2002, Behringer 2007, Sirocko 2013). Early work by Beveridge (1921, 1922) showed historical wheat price data from central Europe to be characterized by cyclic behavior driven by recurring weather conditions (see also discussion in Granger & Hughes 1971). Pfister (1978) confirmed the correlation between grain harvest and price data and pointed to the association of snow cover and rainfall with agrarian productivity and crop yield in selected regions of Switzerland. GP records from Nuremberg and other German cities, reaching back to the 14th century, have been analyzed by Bauernfeind (1993) and later more quantitatively by Bauernfeind & Woitek (1999). These studies revealed a close association between longer-term GP variations and demographic and climatic changes. They also showed that the influence of weather conditions is temporally unstable, but that climate controls increased in the late 16th century compared with earlier periods. Importantly, Bauernfeind (1993) indicated that long-term trends, due to inflation and changing purchasing power, are to be removed from the GP time series to support the evaluation of climate signals inherent to these data. Focusing on years of extremely high prices in the 16th to 18th centuries in the Czech Republic, Brázdil & Durdáková (2000) found that adverse weather conditions in the year and prior year of a harvest explained 2/3 of the variance in local GPs. Zhang et al. (2011) used several economic variables, including European GP data, to corroborate the causal link between climate-driven economic downturns and human crises at continental scales. They also displayed an anti-correlation between GP and temperature data using low-pass filtered time series over the 1200–1800 CE period.

Here, we pursue this line of research by compiling a dataset of 19 historical GP records from Europe and then comparing this network with 2 new, spatially resolved, reconstructions of past temperature (Luterbacher et al. 2016) and drought (Cook et al. 2015).

We removed the lowest-frequency trends from the GP data to account for inflation effects and adjusted the volatility among the records for comparison with the climate reconstructions. We discuss the coherence and aggregation of European GP data, address their correlation with historical famines, and then analyze the significance of drought and temperature signals in the GP network. The influence of drought is analysed after emphasizing the high-frequency interannual variability in the GP time series. Temperature signals are analyzed with emphasis on decadal-scale variability.

2. DATA AND METHODS

2.1. European GP network

A network of 19 historical GP time series from cities in central and northern Europe was compiled (Table 1). The time series cover different periods from the 14th to 18th centuries, with the earliest records starting in 1316 (Exeter), 1348 (Bruges) and 1386 (Strasbourg). Seven records extend to 1800, after which regional supply shocks are considered to cancel out globally due to market integration and free trade (Persson 1999). The common period covered by all 19 GP records is limited to 115 yr (1546–1660) and the average record length is 295 yr. Time series gaps range from 0 to 8.4% and were filled using data from neighboring (and significantly correlating) records, a procedure affecting the statistical independence within the network.

The European GP network covers a region from Madrid (Spain) in the southwest to Gdansk (Poland) in the northeast (Fig. 1). Despite a degree of spatial clustering (e.g. in southern Germany), the network covers reasonably well an area from northern Italy and central Spain in the south, to northern Germany and southern England in the north. A hierarchical cluster analysis of the high-pass filtered GP time series (see ‘Detrending’ below), based on Euclidean distance with the cluster number adopted considering the Ward method (Ward 1963), identified 4 groups: (1) Paris, Tours, Grenoble and Toulouse in the west (hereafter, West cluster); (2) Nuremberg, Augsburg and Wurzburg in the central-south (Cen-S cluster); (3) Strasbourg, Braunschweig, Leiden, Gdansk, Cologne and Xanten in the central-north (Cen-N cluster); and (4) Modena, Siena, Barcelona, Madrid, Exeter and Bruges in the Mediterranean and vicinity of the sea (Peripheral cluster). The Peripheral cluster represents a collection of remaining sites not

Table 1. Historical grain price records from 19 European cities. The data are based on the written record of local sources of the town councils. Many records have already been compiled by R. C. Allen & R. W. Unger (see: www.iisg.nl/hpw/data.php). Other data were digitized for the purpose of this paper

City	Grain	Source	Period	Length	Gaps (%)	Cluster
Augsburg	Rye	Own	1500–1800	290	4.0	Cen-S
Barcelona	Wheat	Allen & Unger	1533–1800	306	–	Peripheral
Braunschweig	Wheat	Own	1513–1800	288	–	Cen-N
Bruges	Wheat	Own	1348–1800	445	2.0	Peripheral
Cologne	Rye	Own	1531–1787	265	–	Cen-N
Exeter	Wheat	Own	1316–1800	457	6.0	Peripheral
Gdansk	Rye	Own	1538–1800	253	4.2	Cen-N
Grenoble	Wheat	Own	1501–1780	275	2.2	West
Leiden	Barley	Allen & Unger	1480–1660	178	2.2	Cen-N
Madrid	Wheat	Allen & Unger	1501–1799	275	8.4	Peripheral
Modena	Wheat	Allen & Unger	1458–1705	248	–	Peripheral
Nuremberg	Rye	Own	1427–1671	245	–	Cen-S
Paris	Wheat	Own	1520–1773	264	–	West
Siena	Wheat	Allen & Unger	1546–1765	220	–	Peripheral
Strasbourg	Barley	Allen & Unger	1386–1792	457	6.6	Cen-N
Toulouse	Wheat	Own	1486–1792	307	–	West
Tours	Wheat	Allen & Unger	1431–1788	358	–	West
Wurzburg	Rye	Own	1500–1799	279	7.4	Cen-S
Xanten	Rye	Own	1500–1800	301	–	Cen-N

closely affiliated with the other cities, but perhaps supported by the commerce of freight through the English Channel and Strait of Gibraltar. The correlation among the peripheral sites is substantially lower ($r = 0.17\text{--}0.29$) compared with the much better confined West, Cen-S and Cen-N clusters ranging from $r = 0.44$ to 0.78 (see the dendrogram in Fig. 1). The

results from the cluster analysis were used to produce 4 mean time series representing regions of coherent GP deviations for comparison with regional summer drought and temperature reconstructions.

2.2. Detrending

The historical GP time series contain (1) a long-term inflation trend ('price revolution') throughout most of the 16th century caused by the influx of gold and silver as well as changing demographic and labor factors (Hamilton 1934, Van der Wee 1978, Kindleberger 1998) and (2) a change from low volatility in the 14th–15th centuries to high volatility in the 17th–18th centuries (Fig. 2). Since both of these

properties are unlikely related to climate, we removed the secular trend and adjusted the volatility using different detrending techniques. A data adaptive power transformation (PT; Cook & Peters 1997) was used to remove volatility changes related to price level (e.g. low volatility and low GP). A 300 yr high-pass filter (300 yr HP) was applied to remove the long-term in-

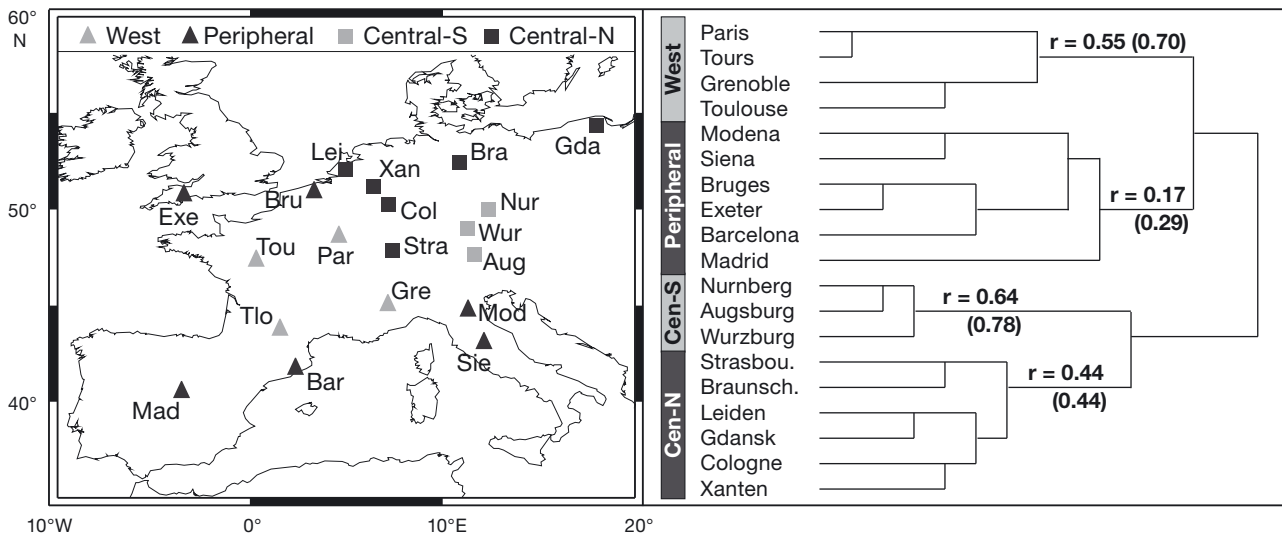


Fig. 1. Location and correlation of historical European grain price (GP) data. Left: The 19 GP data locations (cities) in central and southern Europe. Different symbols and colors indicate the West, Peripheral, Cen-S and Cen-N clusters. Right: Cluster analysis. The r-values indicate correlations among 30 yr high-pass filter (HP) GP time series, values in parentheses are derived from 300 yr HP GP time series. All correlations calculated over the common period 1546–1660 CE (115 yr)

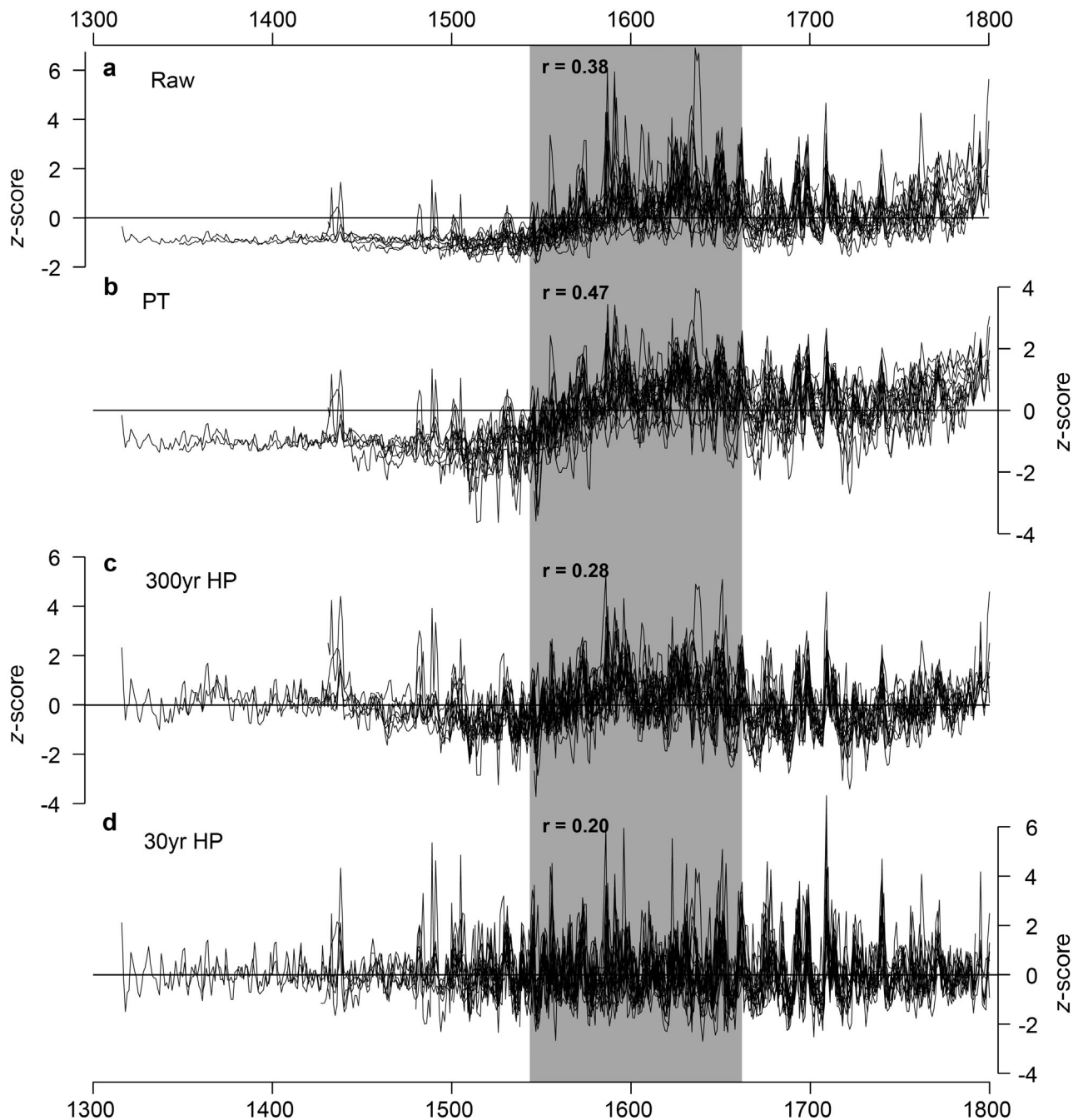


Fig. 2. Raw and detrended grain price (GP) time series. (a) Historical GP data from 19 European cities. Grey bar emphasizes the common period 1546–1660 (115 yr) covered by all time series. r -values indicate the inter-series correlations among the GP data over the common period. (b) Same as in (a), but for the power-transformed (PT) GP series. (c) and (d) Same as in (a), but for the 300 yr high-pass filter (HP) and 30 yr HP filtered data, respectively. All series were normalized to zero mean and one standard deviation

flation trend and emphasize interdecadal-scale variations, and a 30 yr high-pass filter (30 yr HP) was applied to emphasize high-frequency interannual variations in the GP time series. The HP filtered series were computed by calculating ratios between the raw GP values and a smoothing spline of the desired frequency response (Cook & Peters 1981). The resulting

300 yr HP and 30 yr HP time series were used for comparison with spatially resolved drought and temperature reconstructions (Cook et al. 2015, Luterbacher et al. 2016).

Comparison of network mean raw, PT, 300 yr HP and 30 yr HP time series (Fig. 3) not only illustrates the effects of removing low-frequency variance from

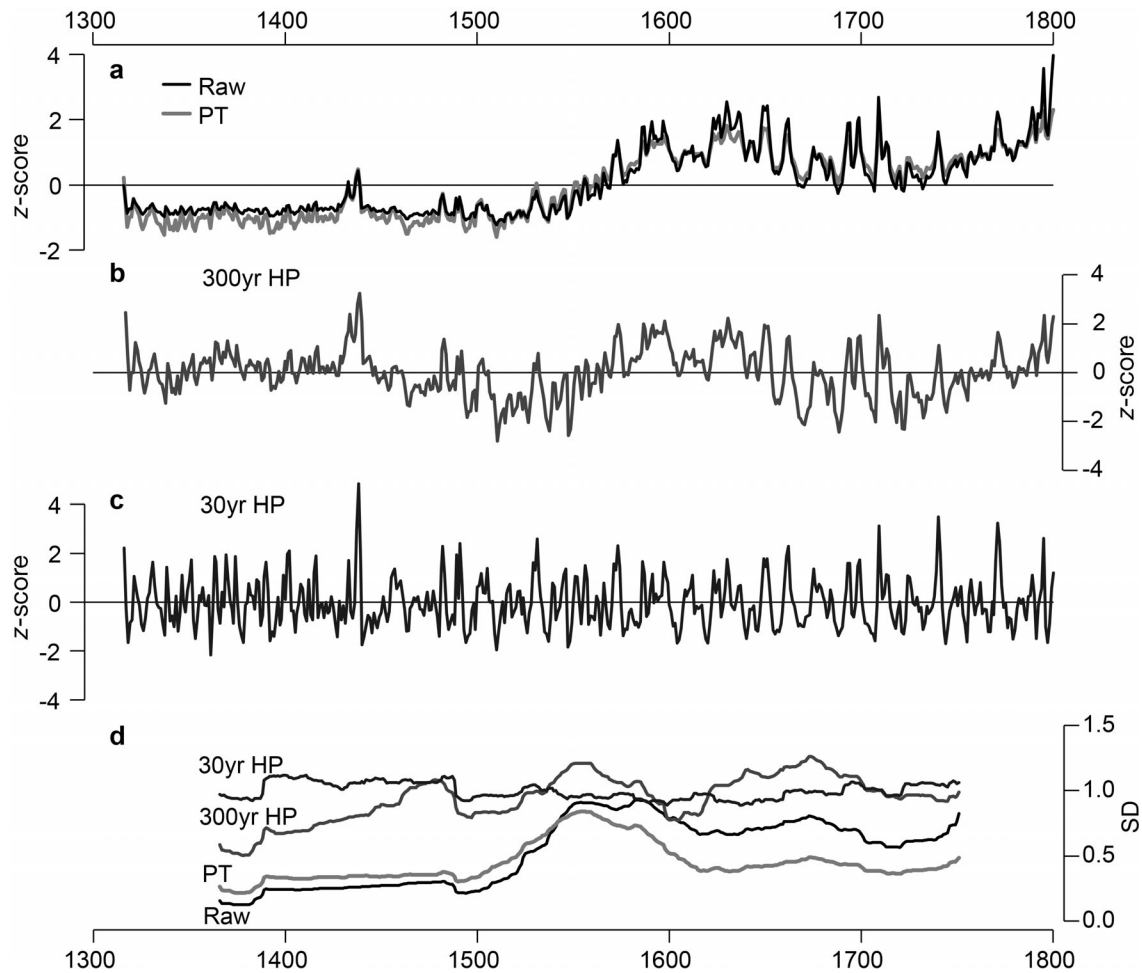


Fig. 3. European mean GP time series. (a) Arithmetic mean of 19 untreated GP time series from Europe (raw) shown together with the mean of the PT series. (b) and (c) Mean time series of the 300 yr HP and 30 yr HP data, respectively. (d) Running standard deviations of the European mean time series calculated in a 100 yr window shifted along the records. See Fig. 2 for abbreviations

the GP records, but also shows how these methods adjust the temporally changing volatility over a ~500 yr period (lowest panel in Fig. 3). PT removed much of the long-term volatility trend, but did not reduce the high variance values in the 16th century. In contrast, the variability of the 300 yr HP mean time series is fairly stable over time, though still contains an obvious increase over the first ~100 yr. The 30 yr HP mean is practically homoscedastic, making these data most suitable for detecting extreme deviations through time and GP correlations with climate reconstructions.

Interestingly, the already significant correlation among the original GP time series ($r = 0.38$, 1546–1660, $p < 0.05$) increases to $r = 0.47$ ($p < 0.01$) after adjusting the time series' variance using PT (Fig. 2b). This value decreases, as expected, after removing the long-term inflation trends in the 300 yr HP data ($r = 0.28$) and further decays to $r = 0.20$ in the 30 yr HP

data, though is still significant at $p < 0.05$ due to the removal of autocorrelation. This latter change between the 300 yr HP and 30 yr HP filtered data indicates that there is common multidecadal-scale variance in the European GP network that is potentially related to external drivers. Climatic fingerprints within the 300 yr HP and 30 yr HP GP networks are assessed at the (1) local scale using the single city GP time series, (2) regional scale using cluster mean time series and (3) continental scale using the mean of all 19 GP series.

2.3. Famines, drought and temperature reconstructions

Before evaluating the potential impact of climate, the sensitivity of the GP network to regional and inter-regional famines from the 14th to 18th centuries (Abel

1972, 1974, Appleby 1979, Jordan 1998, Aberth 2000, Ó Gráda & Chevet 2002, Ó Gráda 2009) was examined. During this period, there are 16 recorded famines (Table 2) ranging from dire crop failures and dearth in 1390 England to severe shortages of food resources and mass mortality between 1771 and 1972 in Germany (Brázdil et al. 2001). The list includes famines that occurred in sub-regions of the GP network (e.g. Spain or France) as well as larger-scale events that likely impacted most of the European continent (e.g. 1437–1440 famine). Famines reported to have lasted longer than 4 yr, included smaller areas, and in regions outside the GP network were not considered. Examples include famines in Venice, Sardinia and Ireland (Engler et al. 2013) and events during 1648–1660 in Poland and the 1670s and 1680s in Spain. To evaluate the significance of famines, we used the 30 yr HP data and the 16 events listed in Table 2 and analyzed the magnitude of GP deviations using superposed epoch

Table 2. Famines in central and southern European countries and regions for the 14th to 18th centuries

Region	Period
England	1390
Europa	1437–1440
Spain	1504
France	1528
Spain	1540
England	1555
England	1586
Spain	1599–1600
England	1623–1624
Spain	1636
France	1650–1652
France	1693–1694
France/Prussia	1709–1710
England	1727–1728
France	1738–1739
Germany	1771–1772

Table 3. Local and regional Palmer drought severity index (PDSI) reconstructions derived from the Old World Drought Atlas (Cook et al. 2015). The atlas' grid resolution is $0.5^\circ \times 0.5^\circ$. Standard deviations and correlations are calculated over the 1400–1800 period using 30 yr HP data. Average correlation is the correlation with all other local and regional PDSI series

	Mean latitude	Mean longitude	No. grid points	Standard deviation	Average correlation	Correlation with Europe
Cen-N	52.53° N	10.40° E	117	1.69	0.51	0.63
Cen-S	48.12° N	12.48° E	114	1.30	0.53	0.59
France	44.79° N	2.74° E	103	1.61	0.58	0.64
Exeter	50.63° N	4.00° W	4	1.75	0.46	0.55
N-Spain	40.77° N	2.49° W	42	1.34	0.15	0.15
Tuscany	44.12° N	11.21° E	12	1.23	0.19	0.20
Europe	48.50° N	21.91° E	5414	0.41	0.46	

analysis (SEA; Panofsky & Brier 1968). In this approach, the GP time series were decomposed into shorter segments of 11 yr and centered around zero in the 5 yr before the famines. SEA was applied to the whole GP network as well as the regionally coherent data, i.e. famines documented in France were compared with the GP West cluster.

Deviations in the GP network were compared with reconstructions of the Palmer drought severity index (PDSI; Palmer 1965) derived from the Old World Drought Atlas (OWDA; Cook et al. 2015). The PDSI is a commonly used indicator of physiological drought ranging from -4 (extremely dry) to $+4$ (extremely moist). The index integrates information on monthly precipitation, temperature and soil water capacity, and is considered effective as a variable to assess crop harvest and failure (Dai et al. 2004, van der Schrier et al. 2006). The OWDA is based on the transfer of tree-ring width and density data into PDSI estimates extending back over the Common Era. Here, we combine several PDSI grid-point reconstructions from the OWDA into means that spatially match the GP clusters (e.g. France), as well as a European mean using all 5414 OWDA grid-point reconstructions (Table 3). Note that the PDSI reconstructions representing larger areas are characterized by reduced standard deviations (see the fifth column in Table 3), a property that needs to be considered when interpreting the severity of drought compared to GP deviations. Also, the seasonality of the drought signal is constrained to June–August and does not capture the potentially important spring months that likely impact grain harvest and prices as well. To assess the significance of the effect of drought variability on historical grain markets, the OWDA-derived PDSI reconstructions were correlated with the 30 yr HP GP time series. In addition, we applied SEA to the GP data considering the 20 driest and 20 wettest recon-

structed summers in Europe from 1500 to 1780 (Table 4). The latter approach was also reversed by applying SEA to the PDSI data considering the 20 highest and 20 lowest GPs.

Since temperature variability is spatially more homogenous than precipitation and drought (Büntgen et al. 2010), we used a summer temperature reconstruction representing southern and central Europe (south of 50° N) derived from the new Luterbacher et al. (2016) network for comparison

Table 4. European-scale extreme PDSI and GP deviations. The 20 lowest and 20 highest reconstructed PDSI and GP values from 1500 to 1780, the period during which the cluster GP time series are represented by ≥ 3 city records (except Cen-S ending in 1671). Drought extremes are derived from PDSI-Europe integrating 5414 grid points (Table 3). All data are 30 yr HP filtered. PDSI data detrended using residuals. GP data normalized

20 lowest PDSI			20 highest PDSI			20 highest GP			20 lowest GP		
No.	Year	PDSI	No.	Year	PDSI	No.	Year	GP	No.	Year	GP
1	1517	-1.04	1	1641	1.16	1	1740	3.59	1	1510	-1.94
2	1718	-0.98	2	1507	1.15	2	1771	3.32	2	1547	-1.82
3	1624	-0.98	3	1663	1.01	3	1709	3.22	3	1744	-1.68
4	1684	-0.94	4	1734	0.95	4	1531	2.66	4	1620	-1.67
5	1719	-0.92	5	1620	0.88	5	1772	2.51	5	1604	-1.66
6	1599	-0.92	6	1510	0.86	6	1573	2.39	6	1755	-1.60
7	1740	-0.87	7	1673	0.81	7	1662	2.37	7	1537	-1.59
8	1572	-0.86	8	1617	0.77	8	1741	2.07	8	1548	-1.58
9	1503	-0.78	9	1712	0.77	9	1661	1.94	9	1707	-1.56
10	1636	-0.77	10	1562	0.74	10	1651	1.86	10	1605	-1.52
11	1659	-0.75	11	1721	0.73	11	1649	1.86	11	1779	-1.50
12	1532	-0.75	12	1682	0.71	12	1630	1.82	12	1619	-1.49
13	1676	-0.74	13	1713	0.70	13	1699	1.81	13	1640	-1.46
14	1746	-0.73	14	1601	0.69	14	1770	1.76	14	1688	-1.36
15	1757	-0.69	15	1754	0.68	15	1586	1.73	15	1576	-1.34
16	1504	-0.65	16	1509	0.66	16	1597	1.71	16	1564	-1.33
17	1610	-0.64	17	1723	0.65	17	1529	1.68	17	1536	-1.29
18	1631	-0.61	18	1751	0.64	18	1694	1.67	18	1706	-1.28
19	1670	-0.59	19	1577	0.63	19	1693	1.67	19	1722	-1.28
20	1666	-0.59	20	1609	0.63	20	1710	1.65	20	1655	-1.27

with the GP data. Luterbacher et al. (2016) developed a spatially resolved ($5^\circ \times 5^\circ$) summer (June–August average) temperature reconstruction back to 755 CE, based on the calibration and transfer of tree-ring and documentary evidence using Bayesian hierarchical modeling (Werner et al. 2013). Here, we correlated the central-southern European reconstruction with the 300 yr HP GP data to assess the influence of summer temperature variability on GP volatility at interannual to multidecadal timescales. Particular attention was given to the Thirty Years' War from 1618 to 1648 and the subsequent 100 yr period to assess potential differences between periods of conflict and tranquility.

3. RESULTS AND DISCUSSION

3.1. GP coherence

The comparison of cluster mean records reveals substantial inter-regional coherence within the European GP network (Fig. 4). The regional GP time series share variance at interannual to interdecadal timescales including a synchronous shift from lower values in the mid-15th to mid-16th centuries, high

values in the late 16th to mid-17th centuries and subsequently lower values again. These low-frequency changes are recorded in all 4 European GP clusters. Their inter-series correlation over the 1431–1792 period (Fig. 4b) is 0.53 and increases to 0.64 after decadal-scale smoothing the GP data.

The high correlations between GP regions in Europe, including the loosely defined Peripheral cluster (see Fig. 1), strongly suggests some large-scale, external driver is operating on the network and regionally synchronizing the GP time series. Some common GP variance could be affected by spatially limited events (e.g. local harvest shocks) that rapidly propagated to other regions through communication and trade, producing large-scale coherent patterns. However, we found no indication of temporally increasing correlations within

and between the regions, as would be expected due to gradually enhancing trade and market integration from the 14th to 18th centuries in Europe. Instead the inter-series correlations declined during the Thirty Years' War (highlighted grey in Fig. 4c) and subsequently increased toward higher values until the mid-18th century.

3.2. Famines and drought

The coincident timing of famines and peaks in the 30 yr HP European GP series (Fig. 5a) suggests a connection between GP and dearth. This association was systematically assessed using SEA, revealing positive GP deviations in most cities centered on the year of famine (lag = 0 on the y axis in Fig. 5b) and insignificant deviations before and thereafter. The GP deviations are larger when the regional cluster data are considered (e.g. famine in France versus GP data from French cities, Fig. 5c) reaching significance at lag = 0 in the Cen-N, Cen-S and West time series. The GP data from the Peripheral cluster, however, do not exceed the 2σ uncertainty range, a finding that potentially reflects the influence of stock management and inter-regional grain trade mitigat-

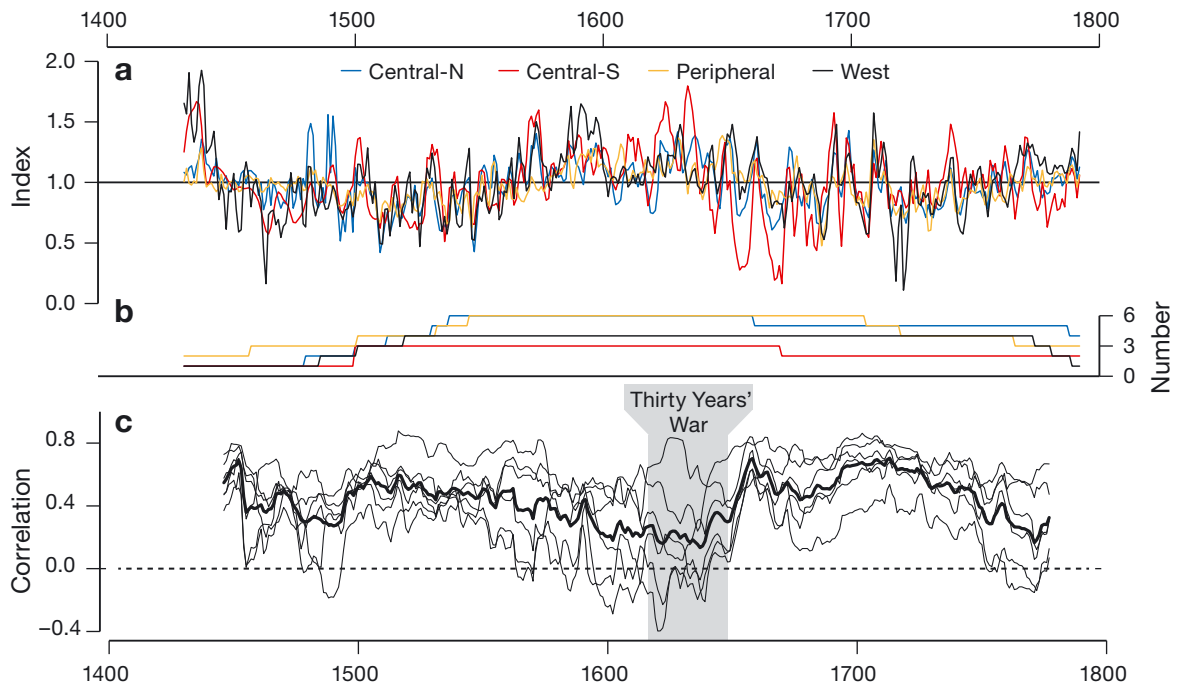


Fig. 4. Coherence of regional GP time series. (a) 300 yr HP GP time series of the Cen-N, Cen-S, Peripheral and West clusters over the common period 1431–1792. (b) Number of single GP series combined in the regional time series. (c) 30 yr running correlations between the regional GP time series (thin curves) and their mean (thick curve). Thirty Years' War from 1618 to 1648 is highlighted in grey. See Fig. 1 for abbreviations

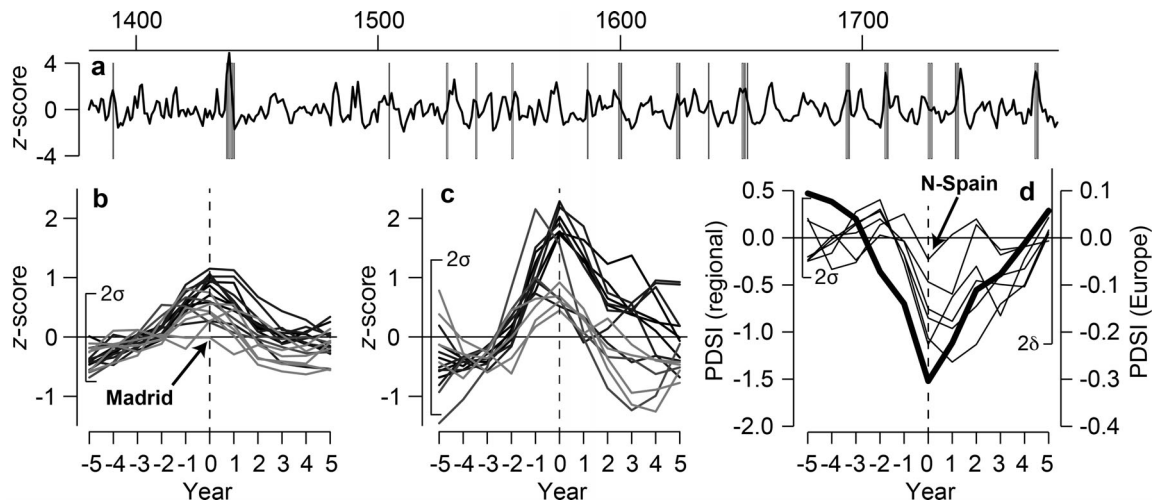


Fig. 5. GP response and PDSI deviations during historical famines. (a) European GP data from 1380 to 1780 (30 yr HP filtered) shown together with 16 major famines in Europe (vertical lines, see Table 2). (b) Superposed epoch analysis (SEA) of the 19 local GP datasets aligned by famines in Europe. Light grey curves are the GP data of the Peripheral cluster, black curves are data from the Cen-N, Cen-S and West clusters. The 2σ uncertainty range is derived from the pre-famine GP variance over the years -5 to -1 . (c) Same as in (b), but for the (much fewer) regionally coherent cases, i.e. only those GP deviations are shown where regional famines (e.g. famine in France) match regional GP data (e.g. GP data from Grenoble, Paris, Toulouse, Tours). (d) Same as in (b), but using the regional (thin curves) and European (bold curve) PDSI data instead of the GP data (see Table 3)

ing the effects of harvest shocks in some of the seaport cities. Admittedly, the limited number of regional famines, the certainly incomplete documentation and the noise inherent to the GP network likely affect these regional differentiations. We also found no

association between famines and volcanic eruptions, as would perhaps be expected based on the impact of such events on large-scale climate (Esper et al. 2013a,b, Schneider et al. 2015, Wilson et al. 2016). Of the 16 famines listed here, only the crisis in 1586

could potentially be related to a major eruption (Kelut on Java, Indonesia). All other famines occurred in years with no obvious volcanic forcing.

Whereas the association between famines and GP has been reported before (Malthus 1798, Ó Grada & Chevet 2002, Campbell 2009, Campbell & Ó Grada 2011), the connection between famines and summer drought in Europe is a novel finding (Fig. 5d). Using the same list of 16 famines (Table 2), distinct negative deviations centered at lag = 0 are seen in the regional PDSI data. Except for the reconstruction from northern Spain, all PDSI estimates exceed the 2σ uncertainty range, revealing a link between summer drought and dearth. This association appears to be independent of regionally changing climate conditions, i.e. it includes sites from dry climates in southern Europe as well as colder and moister climates in central Europe. The figure of low PDSI values centered at lag = 0 is most distinct at the European scale (the bold black curve in Fig. 5d), even though the magnitude of PDSI deviations is much smaller at this large spatial scale, integrating the entire OWDA domain of 5414 grid points (Table 3). The significant PDSI deviation at lag = 0 at the pan-European scale suggests that the European GP and drought networks share variance, a hypothesis tested in the next section.

3.3. GP and summer drought

The correlations between regional GP and PDSI data are negative, indicating a link between high (low) prices and dry (wet) summers. The coefficients generally increase when removing low-frequency variance (using the 30 yr HP GP data), though overall hardly reach $r = -0.2$ ($p < 0.01$). The correlation pat-

terns appear more meaningful when comparing results after temporally shifting the time series by up to 10 yr (lags 0–10 in Fig. 6).

The correlations between local GP and PDSI data are not coherent; they include outliers (e.g. Exeter) and various coefficients that hardly differ from zero (Fig. 6a). The fact that negative correlations extend beyond lags 1 and 2 indicates that there is memory in the relationship between PDSI and GP, i.e. growing-season drought conditions influence GPs beyond the current year's harvest. Both of these characteristics—the negative correlation coefficients and the memory effects—are also noticeable when comparing the drought estimates with the European mean GP time series (Fig. 6b). Maximum correlation is seen between the European PDSI and GP time series ($r = -0.21$ at lag 0, $p < 0.01$), a finding that underscores (1) the importance of large-scale drought/pluvial events on grain harvest, (2) the likely influence of inter-regional trade and market integration on GP patterns, and (3) an improved common signal when integrating multiple grid-point PDSI reconstructions over larger areas (in this case the full OWDA domain; Cook et al. 2015).

The influence of dry and moist summer conditions on European GPs is explicit if only the most negative and positive PDSI deviations are considered (Table 4). Plotting these events on top of the European mean illustrates a close relationship between high GPs and extremely dry summers, as well as low GPs and extremely moist summers (Fig. 7a). However, the application of SEA to the city and cluster GP data reveals spatially variable drought responses (Fig. 7b–e). In particular, the Mediterranean cities Barcelona and Siena (Fig. 7b) show no reaction in dry years, contradicting the expectation of increased drought sensitivity of southern grain markets. In

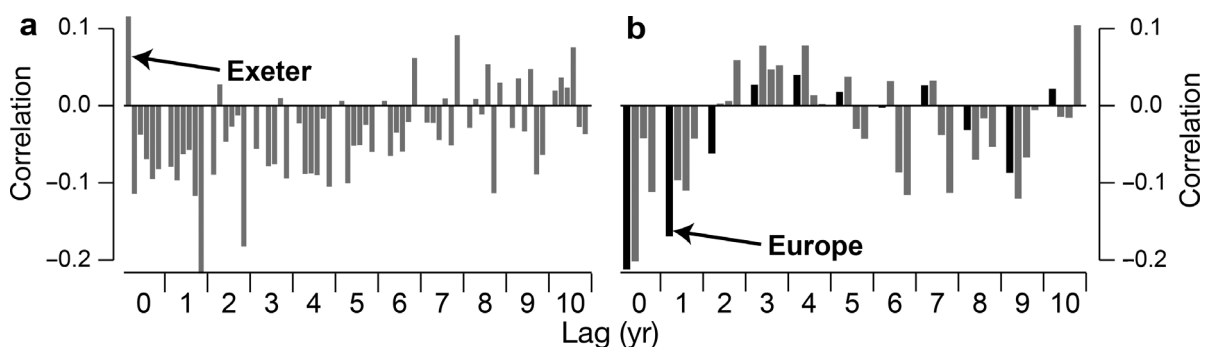


Fig. 6. Correlation between GP and PDSI data. (a) Lag 0 to lag 10 correlations between regional PDSI and regional 30 yr HP GP data (e.g. French GP vs. French PDSI time series) over the period 1500–1780 (except Cen-S ending in 1671). (b) Lag 0 to lag 10 correlations between regional PDSI data (including Europe, see Table 3) and European-scale GP data, i.e. the mean of all 19 city GP time series. Black bars indicate the correlations between the European-scale PDSI and European-scale GP data

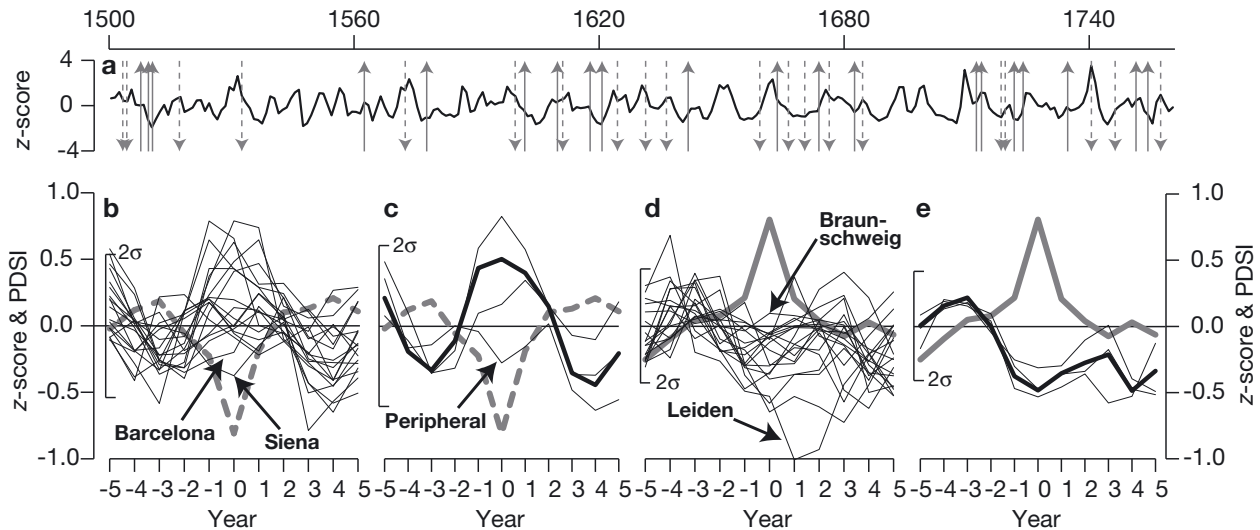


Fig. 7. GP deviations during extremely dry and wet years. (a) European GP data (30 yr HP filtered) shown together with the 20 driest (dashed downward arrows) and 20 wettest (solid upward arrows) reconstructed summers in Europe over the 1500–1780 period (see Table 4). (b) Superposed epoch analysis (SEA) of the 19 local GP datasets (black curves) aligned by the 20 driest summers (grey dashed curve is the mean PDSI). (c) Same as in (b), but for the regional GP time series (except for the shorter Cen-S cluster series) and the European mean (bold black curve). (d) SEA of the 19 local GP datasets (black) aligned by the 20 wettest summers (grey curve). (e) Same as in (d), but for the regional GP time series (thin black) and the European mean (bold black curve)

addition, there are city records with a response that does not deviate substantially from zero (e.g. Braunschweig highlighted in Fig. 7d), or does not exceed the 2σ uncertainty range at lag 0.

The influence of hydroclimatic extremes is most obvious at the cluster-mean and pan-European scales. At these spatial scales, only the Peripheral GP cluster appears to be insensitive to widespread summer drought, which is potentially related to mitigating effects of ship trading on these markets. This hypothesis cannot be supported by written documentation of grain trade through the Strait of Gibraltar, however. In addition, the seasonal constraint of the OWDA to summer (June–August) drought likely adds to the low correlations, as the potentially important winter and spring months are not captured by the network (Cook et al. 2015). However, the European GP data produce distinct patterns deviating by $+0.50$ SD in the 20 driest summers (PDSI = -0.81) and -0.48 SD in the 20 wettest summers (PDSI = $+0.81$; see the bold curves in Fig. 7c and e). Even if the drought signals were expected to be stronger (Stone 2014), particularly after discerning the famine–drought association (Fig. 5d), the clear tendency toward higher GPs centered on dry years and lower GPs centered on wet years is in some sense also astonishing, given the severe changes in market integration and liberalization documented over the 14th to 18th centuries (Van der Wee 1978, Persson

1999). These processes included a rise in market-driven agriculture, commercialization of peasants, advancement of stock management and trade, and regionally varying population growth and decline. In light of these changes, any large-scale association between GP and climate variability might appear surprising.

3.4. GP and temperature

In contrast to the drought–GP comparison, where the correlations generally increased when the low-frequency variance was removed, the reconstructed temperatures seem to additionally cohere at interdecadal timescales with the GP data. A comparison of the 300 yr HP cluster mean series with reconstructed central-southern European summer temperatures reveals synchronous high- to low-frequency fluctuations (Fig. 8, temperatures inverted). Low GPs in the 15th and early 16th centuries cohere with a period of high summer temperatures, cold conditions in the late 16th and early 17th centuries cohere with high GPs, and subsequently lower GPs are again accompanied by warmer temperatures. This association is also reflected in the uniform correlations between summer temperatures and the Cen-N ($r = -0.25$), Peripheral ($r = -0.25$), West ($r = -0.26$) and Cen-S ($r = -0.28$) clusters over the 1500–1780 period (all $p < 0.01$). The cor-

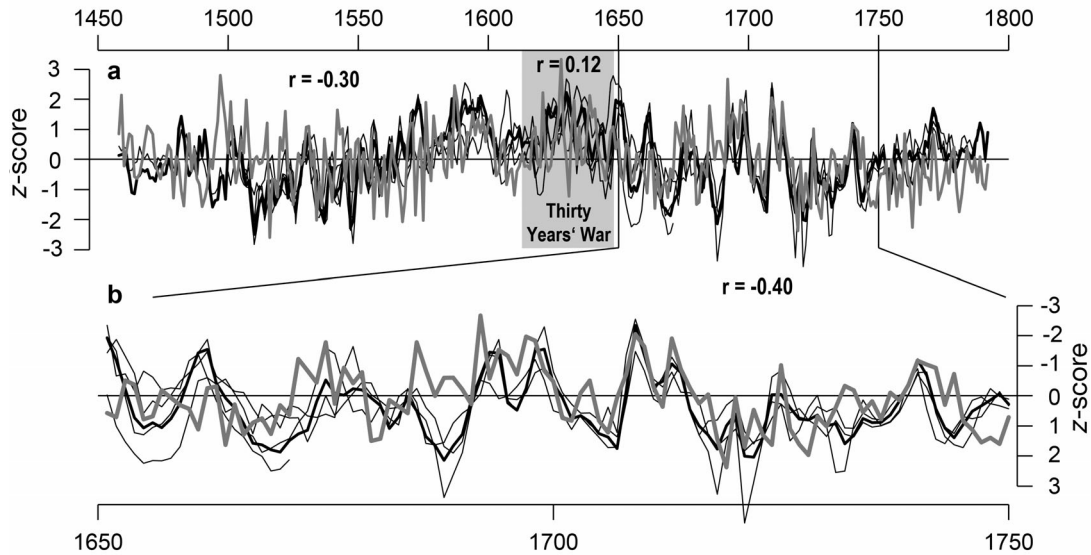


Fig. 8. Coherence between historical GP and reconstructed temperature data. (a) Regional GP time series of the Cen-N, Cen-S, Peripheral and West clusters (thin black curves, 300 yr HP) and their mean (bold black curve) plotted together with the reconstructed summer temperatures from central and southern Europe (grey curve, Luterbacher et al. 2016). Note that the temperature data have been reversed, i.e. high values indicate cold conditions. Correlations refer to the 1500–1780 period ($r = -0.30$) covered by ≥ 3 regional GP series, and the 1618–1648 Thirty Years' War period ($r = 0.12$). (b) Zoom-in over the 1650–1750 period ($r = -0.40$)

relation increases to $r = -0.30$ for the European mean GP time series (black bold curve in Fig. 8; $p < 0.001$), indicating a close match between price and temperature variability at sub-continental scales.

Common low-frequency variance between the temperature and GP data is further substantiated by the increased correlations with the 10 yr low-pass filtered time series, reaching $r = -0.47$ for Cen-N (min.) and $r = -0.60$ for Cen-S (max.) over the 1500–1780 period. Whereas this finding seems to reinforce an important link between a major socioeconomic variable and climate over an extended historical period, the reduced degrees of freedom due to the substantially increased autocorrelation limits the statistical significance of this result ($p \approx 0.1$). However, both the correlations using original and smoothed data suggests that GPs were higher during cold periods and lower during warm periods, and that this association holds true for larger regions in central and southern Europe. For the northern markets, this result is not surprising as harvest shocks (high GP) typically coincide with below-average growing-season temperatures. For the southern markets, however, harvest shocks were originally hypothesized to coincide with warm, and typically dry, growing-season conditions. The spatially coherent response structure encompassing Gdansk and Exeter in temperate central Europe, as well as Barcelona and Siena in the Mediterranean, clearly contradicts this presumption, but

demonstrates an analogous (negative) temperature correlation throughout the European GP network.

Whereas the GP–climate correlations are fairly homogeneous among the regional clusters, substantial temporal fluctuations are noticeable. Most striking, the otherwise negative correlation over the full 1500–1780 period (see above, $r = -0.3$ at the European scale) weakens during the early 17th century and even turns positive ($r = 0.12$) during the Thirty Years' War, a sustained period of conflict from 1618 to 1648 in parts of Europe, except for the West cluster and sites in Spain. Interestingly, not only do the GP–temperature correlations disappear during this period, but also the inter-correlation among GP clusters substantially weakens, reaching an unprecedented low of only $r = 0.17$ centered in 1633 (see running correlations in Fig. 4b). It seems obvious that the conflict over political preeminence and religion not only limited the exchange of goods and price coherence in Europe, but also decoupled the GP variability from its climate forcing. Subsequent to the Thirty Years' War, the correlation between reconstructed summer temperatures and historical GPs increased to $r = -0.4$ ($p < 0.01$) over the 1650–1750 period (Fig. 4b), defining a marked difference between wartime and peacetime GP–climate interaction.

Both the large-scale coherent GP patterns and the temporally changing GP–climate correlations were not readily expected when compiling the European

GP network. The 14th to 18th century period analyzed here encompasses fundamental transitions in market liberalization and transport. Crop production and stock management changed radically, regional and large-scale conflict alternated with periods of quietude, and fluctuating population numbers severely affected crop demand and supply. Such circumstances strongly argue for spatially restricted analyses of historical GPs at regional and even local scales (Pfister & Brázdil 2006). However, large-scale analyses offer the chance to identify common deviations and trends that would otherwise remain unnoticed in local studies and assessments of single events. From this perspective, the herein identified inter-regionally coherent GP patterns, their temporal change, as well as the varying GP–climate associations are important characteristics of the exchange of goods in 14th to 18th century Europe.

4. CONCLUSIONS

A continental-scale network integrating GP data from 19 cities in central and southern Europe was compiled to evaluate the impact of climate variability on historical grain markets. The GP time series were detrended to remove long-term inflation and volatility trends, and to homogenize interannual- to inter-decadal-scale variability. The detrended data revealed substantial correlations among European cities and regions, but appeared unaffected by long-term trends of augmented market integration, i.e. the inter-regional GP correlations do not increase over the 14th to 18th centuries. In fact, the European GP time series were spatially less coherent during the Thirty Years' War (1618–1648), but correlated better before and after. This finding questions the significance of changing transport costs and liberalization effects on historical GP variations (Persson 1999), though these central characteristics of market integration are perhaps preserved in the volatility changes that were originally removed to analyze climate-induced GP variance.

The climatic fingerprints on the European GP network were assessed using spatially resolved summer temperature and drought reconstructions that have recently been developed by international teams of paleoclimatologists (Cook et al. 2015, Luterbacher et al. 2016). Comparisons between the regional GP time series and reconstructed PDSI estimates returned weak but significant correlations ($r = -0.2$), and only marginally enhanced results if the 20 driest and 20 wettest summers of the 1500–1780 period were con-

sidered. Surprisingly, the drought response was not strongest at the local scale, but increased when both the GP and PDSI data were averaged at the continental scale. In addition, the negative correlation between GP and PDSI data (i.e. high prices coincide with dry conditions) recorded in the northern portion of the GP network, did not increase toward southern Europe. This finding contradicted our expectation of intensified hydroclimatic control over Mediterranean GPs where harvest shocks and market failures were anticipated to be primarily driven by drought events. In the coastal Mediterranean cities (Barcelona, Modena and Siena), drought effects might be mitigated by reliance on shipping connecting these sites with the western European markets in Exeter and Bruges. Long-distance trade between these peripheral sites potentially decoupled the GP–climate relationships, making these markets less vulnerable to harvest shocks due to regional drought.

In contrast to the overall weak GP–drought response, reconstructed summer temperatures were found to correlate better (up to $r = -0.3$ over the 1500–1780 period and $r = -0.6$ after decadal smoothing) with historical GP fluctuations. As with the PDSI, the correlations increased if both the GP and temperature estimates were integrated at the European scale, which is supported by the increased spatial covariance of temperature, compared with the more heterogeneous drought variability (Büntgen et al. 2010). The reconstructed summer temperatures cohered well with GP changes at lower frequencies, including low prices and warm conditions in the early 16th and 18th centuries, and high prices and cold conditions in the late 16th and early 17th centuries. The temperature–GP correlations completely fell apart during the Thirty Years' War (1618–1648), but increased to $r = -0.40$ over the subsequent 1650–1750 period, in line with the temporally changing coherence among the European GP sites during wartime and peacetime. This finding of increased temperature control of crop harvest and synchronized GPs during periods of quietude, fading during periods of conflict, appears to be fairly robust throughout the European network analyzed here, even if the impact of the Thirty Years' War was certainly less immediate in the West and Peripheral sites of the GP network. Further testing of the validity of this conclusion could be supported by compiling an even denser GP network. The assessment of spatio-temporal characteristics of social vulnerability to climate, however, requires a careful removal of long-term volatility and inflation trends that are most likely unrelated to climate.

Acknowledgements. This study was supported by the German Science Foundation, Grant # 161/9-1 'Development of density chronologies for eastern and southern Europe'. We thank Jakob Eggert and Maria Mischel for digitizing grain price data and databank compilation.

LITERATURE CITED

- Abel W (1972) Massenarmut und Hungerkrisen im vorindustriellen Deutschland. Vanderhoeck und Ruprecht, Göttingen
- Abel W (1974) Massenarmut und Hungerkrisen im vorindustriellen Europa. Versuch einer Synopsis. Paul Parey, Hamburg
- Aberth J (2000) From the brink of the apocalypse. Confronting famine, plague, war and death in the later middle ages. Routledge, London
- ✦ Allen RC (2001) The great divergence in European wages and prices from the middle ages to the first world war. *Explor Econ Hist* 38:411–447
- ✦ Appleby AB (1979) Grain prices and subsistence crises in England and France, 1590–1740. *J Econ Hist* 39:865–887
- Bauernfeind W (1993) Materielle Grundstrukturen im Spätmittelalter und der frühen Neuzeit, Preisentwicklung und Agrarkonjunktur am Nürnberger Getreidemarkt von 1339 bis 1670. Universitätsbuchhandlung Korn und Berg, Nürnberg
- ✦ Bauernfeind W, Woitek U (1999) The influence of climatic change on price fluctuations in Germany during the 16th century price revolution. *Clim Change* 43:303–321
- Behringer W (2007) Kulturgeschichte des Klimas. Von der Eiszeit bis zur globalen Erwärmung. CH Beck, München
- ✦ Beveridge WH (1921) Weather and harvest cycles. *Econ J* 31:429–452
- Beveridge WH (1922) Wheat prices and rainfall in Western Europe. *JR Stat Soc* 85:412–475
- Braudel F, Spooner F (1967) Prices in Europe from 1450 to 1750. In: Rich EE, Wilson CH (eds) Cambridge economic history of Europe 4. Cambridge University Press, Cambridge, p 374–486
- Brázdil R, Durdáková M (2000) The effect of weather factors on fluctuations of grain prices in the Czech Lands in the 16th–18th centuries. *Prace Geograficne* 108:19–25
- Brázdil R, Valásek H, Luterbacher J, Macková J (2001) Hungerjahre 1770–1772 in den Böhmischesen Ländern: Verlauf, meteorologische Ursachen und Auswirkungen. *Österr Z Gesch* 2:44–78
- ✦ Büntgen U, Franke J, Wilson R, González-Rouco F, Esper J (2010) Assessing the spatial signature of European climate reconstructions. *Clim Res* 41:125–130
- Campbell BS (2009) Four famines and a pestilence: harvest, price, and wage variations in England, 13th to 19th centuries. In: Liljewall B, Flygare IA, Lange U, Ljunggren L, Söderberg J (eds) Agrarian history many ways: 28 studies on humans and the land. KSLAB, Stockholm, p 23–56
- ✦ Campbell BMS, Ó Gráda C (2011) Harvest shortfalls, grain prices, and famines in preindustrial England. *J Econ Hist* 71:859–886
- ✦ Cook ER, Seager R, Kushnir Y, Briffa KR and others (2015) Old World megadroughts and pluvials during the Common Era. *Sci Adv* 1:e1500561
- Cook ER, Peters K (1981) The smoothing spline: a new approach to standardizing forest interior tree-ring width series for dendroclimatic studies. *Tree-Ring Bull* 41:45–53
- ✦ Cook ER, Peters K (1997) Calculating unbiased tree-ring indices for the study of climatic and environmental change. *Holocene* 7:361–370
- ✦ Dai A, Trenberth KE, Qian T (2004) A global dataset of Palmer drought severity index for 1870–2002: relationship with soil moisture and effects of surface warming. *J Hydrometeorol* 5:1117–1130
- ✦ de Vries J (1980) Measuring the impact of climate on history: the search for appropriate methodologies. *J Interdiscip Hist* 10:599–630
- ✦ Engler S, Mauelshagen F, Werner J, Luterbacher J (2013) The Irish famine of 1740–1741: causes and effects. *Clim Past* 9:1161–1179
- ✦ Esper J, Büntgen U, Luterbacher J, Krusic P (2013a) Testing the hypothesis of post-volcanic missing rings in temperature sensitive dendrochronological data. *Dendrochronologia* 31:216–222
- ✦ Esper J, Schneider L, Krusic PJ, Luterbacher J and others (2013b) European summer temperature response to annually dated volcanic eruptions over the past nine centuries. *Bull Volcanol* 75:736
- Glaser R (2002) Klimageschichte Mitteleuropas. 1200 Jahre Wetter, Klima, Katastrophen. Wissenschaftliche Buchgesellschaft, Darmstadt
- ✦ Granger CWJ, Hughes AO (1971) A new look at some old data: the Beveridge wheat price series. *JR Stat Soc A* 134: 413–428
- Hamilton EJ (1934) American treasure and the price revolution in Spain. Harvard University Press, Cambridge
- Jordan WC (2000) The great famine. Northern Europe in the early fourteenth century. Princeton University Press, Princeton, NJ
- Kindleberger CP (1998) Economic and financial crises and transformations in sixteenth-century Europe. *Essays in International Finance* 208. Department of Economics, Princeton University, Princeton, NJ
- ✦ Luterbacher J, Werner JP, Smerdon JE, Fernández-Donado L and others (2016) European summer temperatures since Roman times. *Environ Res Lett* 11:024001
- Malthus TR (1798) An essay on the principle of population, as it affects the future improvement of society. Johnson, London
- ✦ Ó Gráda C, Chevet JM (2002) Famine and market in ancien régime France. *J Econ Hist* 62:706–733
- Ó Gráda C (2009) Famine. A short history. Princeton University Press, Princeton, NJ
- Palmer WC (1965) Meteorological drought. Research Paper 45, US Department of Commerce, Washington, DC
- Panofsky HA, Brier GW (1968) Some applications of statistics to meteorology. Penn State University Press, University Park, PA
- Persson KG (1999) Grain markets in Europe, 1500–1900. Cambridge University Press, Cambridge
- ✦ Pfister C (1978) Climate and economy in eighteenth-century. *J Interdiscip Hist* 9:223–243
- ✦ Pfister C, Brázdil R (2006) Social vulnerability to climate in the 'Little Ice Age': an example from Central Europe in the early 1770s. *Clim Past* 2:115–129
- Pfister U, Uebele M, Albers H (2011) The great moderation of grain price volatility: market integration vs. climatic change, Germany, seventeenth to nineteenth centuries. BETA-Workshop in Historical Economics, Strasbourg, 13–14 May 2011, University of Strasbourg
- Post JD (1985) Food shortage, climatic variability, and epidemic disease in pre-industrial Europe: the mortality peak

- in the early 1740s. Cornell University Press, New York, NY
- ✦ Schneider L, Smerdon J, Büntgen U, Wilson R, Myglan VS, Kirilyanov A, Esper J (2015) Revising midlatitude summer temperatures back to A.D. 600 based on a wood density network. *Geophys Res Lett* 42:4556–4562
- Sirocko F (2013) *Geschichte des Klimas*. Theiss, Stuttgart
- ✦ Söderberg J (2006) Grain prices in Cairo and Europe in the Middle Ages. *Res Econ Hist* 24:189–216
- ✦ Stone D (2014) The impact of drought on early fourteenth-century England. *Econ Hist Rev* 67:435–462
- ✦ van der Schrier G, Briffa KR, Jones PD, Osborn TJ (2006) Summer moisture variability across Europe. *J Clim* 19: 2818–2834
- ✦ Van der Wee H (1978) Prices and wages as development variables: a comparison between England and the southern Netherlands, 1400–1700. *Acta Hist Neerlandica* 10:58–78
- ✦ Ward JH Jr (1963) Hierarchical grouping to optimize an objective function. *J Am Stat Assoc* 58:236–244
- ✦ Werner JP, Luterbacher J, Smerdon JE (2013) A pseudo-proxy evaluation of Bayesian hierarchical modelling and canonical correlation analysis for climate field reconstructions over Europe. *J Clim* 26:851–867
- ✦ Wilson RJS, Anchukaitis K, Briffa KR, Büntgen U and others (2016) Last millennium Northern Hemisphere summer temperatures from tree rings. Part I: the long term context. *Quat Sci Rev* 134:1–18
- ✦ Zhang DD, Lee HF, Wang C, Li B, Pei Q, Zhang J, An Y (2011) The causality analysis of climate change and large-scale human crisis. *Proc Natl Acad Sci USA* 108: 17296–17301

*Editorial responsibility: Toshichika Iizumi,
Tsukuba, Japan*

*Submitted: June 6, 2016; Accepted: December 6, 2016
Proofs received from author(s): March 16, 2017*